

# Room temperature ferroelectric properties and leakage current characteristics of $\text{Bi}_2\text{FeMnO}_6/\text{SrTiO}_3$ bilayered thin films by chemical solution deposition

L. M. Shen, X. G. Tang\*, Q. X. Liu, Y. P. Jiang, Y. G. Wang, and W. P. Li

School of Physics and Optoelectric Engineering, Guangdong University of Technology, Guangzhou, Guangdong 510090, P. R. China

Received 4 December 2013, revised 11 February 2014, accepted 12 February 2014

Published online 11 March 2014

**Keywords** chemical solution deposition, double-perovskite, ferroelectrics, leakage current, thin films

\* Corresponding author: xgtang6@yahoo.com, Phone: +86 20 3932 2265, Fax: +86 20 39322265

$\text{Bi}_2\text{FeMnO}_6/\text{SrTiO}_3$  (BFMO/STO) bilayered thin films were grown on  $\text{LaNiO}_3$  (LNO) buffered Si(100) substrate by chemical solution deposition. The structure and surface morphology of the bilayered thin films have been characterized by X-ray diffraction and atomic force microscopy. The Au/BFMO/STO/LNO thin-film capacitor showed well-saturated hysteresis loop at an applied field of  $330 \text{ kV cm}^{-1}$  with remnant polarization ( $2P_r$ ) and coercive electric field ( $2E_c$ ) values of  $1.3 \mu\text{C cm}^{-2}$  and  $80 \text{ kV cm}^{-1}$ , respectively. The films show

leakage current density in the order of  $10^{-5} \text{ A cm}^{-2}$  in the whole electric field region. The leakage current depended on the voltage polarity. The Au/BFMO/STO interface forms an Ohmic contact with Au electrode biased negatively. At low electric field, the BFMO/STO/LNO interface forms an Ohmic contact with LNO electrode biased negatively. A further increase of applied electric field, the conduction shows a space-charge-limited-current behavior.

© 2014 WILEY-VCH Verlag GmbH & Co. KGaA, Weinheim

**1 Introduction** Ferroelectric materials, which have a reversible spontaneous polarization, have wide applications in nonvolatile random access memory devices, transducers and sensors [1–3]. A recent focus in this area is the double-perovskite structured ( $\text{A}_2\text{BB}'\text{O}_6$ ) ferroelectrics [4–6]. It was theoretically designed for new potential applications and to improve the disadvantages of perovskite ferroelectrics. The disadvantages such as large leakage current and low temperature ferroelectricity limit its applications. Especially, only a few studies on pure double-perovskite  $\text{Bi}_2\text{FeMnO}_6$ , because it is difficult to be fabricated due to the metastable state. Few earlier researches focused on the growth of  $\text{Bi}_2\text{FeMnO}_6$  film by pulsed laser deposition or electrospray method and verifying its magnetic properties, which found to be weak ferromagnetic at both low and room temperature [7–9]. Moreover, low temperature ferroelectric properties and magnetic properties also are found in  $\text{Bi}_2\text{FeMnO}_6/\text{CaRuO}_3$  heterostructures at 250 K and in  $\text{Bi}_2\text{FeMnO}_6$  thin films at 200 K [10, 11], respectively.

However, there is few report on chemical deposition-derived double-perovskite thin films and it is a challenge to fabricate thus pure thin films with room temperature ferroelectricity because of the large leakage current [12]. It is well known that chemical-derived  $\text{BiFeO}_3$  based thin films always show relatively poor leakage characteristics, which is likely attributed to the presence of oxygen vacancies or valence fluctuation of iron between  $\text{Fe}^{3+}$  and  $\text{Fe}^{2+}$ .  $\text{SrTiO}_3$  is a traditional good insulator, which is chosen to improve the leakage property of  $\text{Bi}_2\text{FeMnO}_6$  film.

Different from the previous studies, in this work,  $\text{Bi}_2\text{FeMnO}_6/\text{SrTiO}_3$  bilayered thin films were first synthesized on  $\text{LaNiO}_3$  buffered Si(100) substrate by a simple chemical solution deposition (CSD) process. The results show the room-temperature ferroelectric properties and low leakage current density.

**2 Experimental procedure** The  $\text{Bi}_2\text{FeMnO}_6$  (BFMO)/ $\text{SrTiO}_3$  (STO) bilayered thin films were prepared

on LaNiO<sub>3</sub> (LNO) buffered Si(100) substrate by a CSD. The STO and LNO thin layers prepared by chemical precursor solutions were described in previous literatures [13, 14]. The preparation for BFMO precursor solution could be described as follows. Reagent-grade bismuth nitrate [Bi(NO<sub>3</sub>)<sub>3</sub> · 5H<sub>2</sub>O], manganese acetate [C<sub>4</sub>H<sub>6</sub>MnO<sub>4</sub> · 4H<sub>2</sub>O], and iron nitrate [Fe(NO<sub>3</sub>)<sub>3</sub> · 9H<sub>2</sub>O] were used as raw materials, and glacial acetic acid CH<sub>3</sub>COOH was selected as solvent. In order to compensate the Bi loss during annealing process, additional bismuth nitrate (5 mol%) was added during the preparation of the solution [15]. Bismuth nitrate, iron nitrate, and manganese acetate were mixed with a proper molar ratio (Bi:Fe:Mn = 2.1:1:1) and dissolved in glacial acetic acid, respectively. Meanwhile, acetyl acetone was added to stabilize the solution. Then, the mixed solutions were stirred at 60 °C for more than 4 h, until the concentration of the final solution was adjusted to 0.2 mol L<sup>-1</sup>. The depositions were carried out by spin coating at 3000 rpm for 30 s. After every coating, the films were heated in air at 300 °C for 30 min on a hot plate. After finished coatings, the thin films were annealed at 600 °C for 15 min by rapid thermal annealing (RTA).

The thickness of the as-grown thin films on Si(100) substrate was measured by a Tencor P-10 surface profiler (KLA-Tenor Corporation, USA). The thickness of LNO bottom electrode layer is 50 nm. The thickness of BFMO and STO on LNO/Si substrate was about 100 and 50 nm, respectively. For electrical measurements, top gold (Au) electrodes of 0.2 mm diameter were deposited through a shadow mask onto the BFMO thin films by a vacuum evaporation. The structure of the film was determined by X-ray powder diffraction (Pgeneral XD-2, China) with Cu K $\alpha$  radiation. The surface morphology and roughness of the BFMO/STO bilayered thin films were determined by atomic force microscopy (CSPM5500, Ben Yuan, China) using tapping mode amplitude model. Both the ferroelectric properties and leakage current characteristics were measured by Radiant Technologies Precision Premier II (Radiant Tech, USA) at room temperature.

### 3 Results and discussion

Figure 1 shows the X-ray diffraction (XRD) pattern of the BFMO/STO bilayered thin films on LNO buffered Si(100) substrate. As determined by first principles calculations, BFMO is a metastable compound due to the positive formation enthalpy. It has also been reported that the BFMO metastable phase structure, crystallizing with different space groups, depends on the nature of the deposition method [7, 16]. In this work, we firstly tried a conventional CSD method and STO was selected as a good insulator. No diffraction peaks for STO were observed on LNO buffered Si(100) substrate. Therefore, six peaks, (002), (102), (110), (004), (116), and (008) were observed in the XRD pattern of the BFMO/STO bilayered thin films which suggests a polycrystalline hexagonal perovskite structure with P6<sub>3</sub>cm space-group [17–20]. The relative peak intensity of  $I(00l)/I(hkl)$  is calculated to be 0.56, and the highest peak is the (004), suggesting

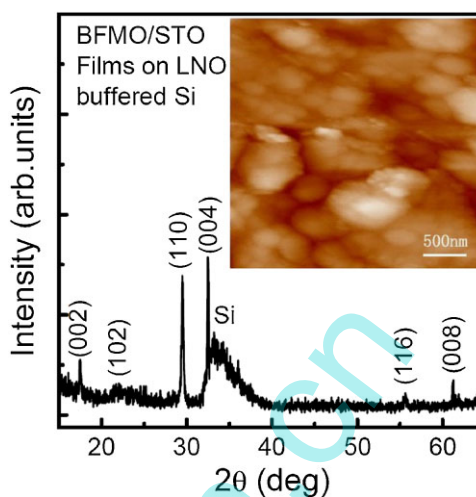


**Figure 1** XRD pattern of BFMO/STO bilayered thin film grown on the LNO buffered Si(100) substrate. Inset shows the AFM images of the BFMO/STO bilayered thin films.

slightly preferred (001)-orientation growth for the BFMO/STO bilayered thin films on LNO layer. The hexagonal perovskite structure was also observed in the hydrothermal prepared ErMnO<sub>3</sub> and TmMnO<sub>3</sub> powder crystals [17], in high-pressure synthesized RMnO<sub>3</sub> (R = Sc, Dy~Lu) samples [18], in rf magnetron sputtering deposition BiMnO<sub>3</sub> and BiFe<sub>0.5</sub>Mn<sub>0.5</sub>O<sub>3</sub> films [19], and in atomic layer deposition YMnO<sub>3</sub> thin films [20], respectively.

Inset shows the surface morphology of the BFMO/STO bilayered thin films grown on a LNO buffered Si (100) substrate, which exhibits a dense microstructure with no cracks and voids. The root mean square (RMS) roughness of the BFMO/STO bilayered thin films is about 14.5 nm. And typically protrusions or small coalescent granular structures are seen on the surface of the sample, which are composed of spherical grains around 280 nm in size.

Figure 2 shows the  $P$ - $E$  hysteresis loop recorded with a 50 Hz triangle wave signal at room temperature for the

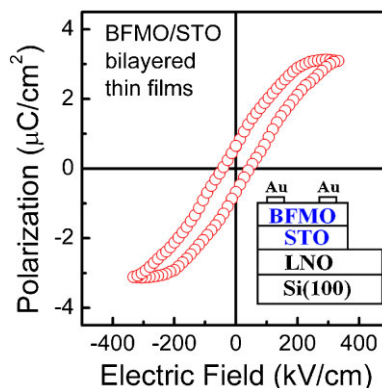
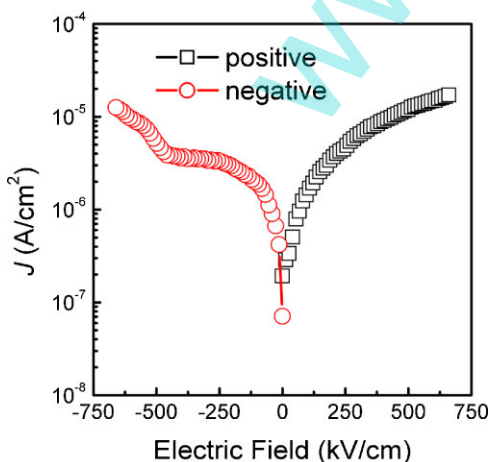


**Figure 2**  $P$ - $E$  hysteresis loop of Au/BFMO/STO/LNO thin-film capacitor. The inset shows the schematic illustration of the thin-film capacitor.

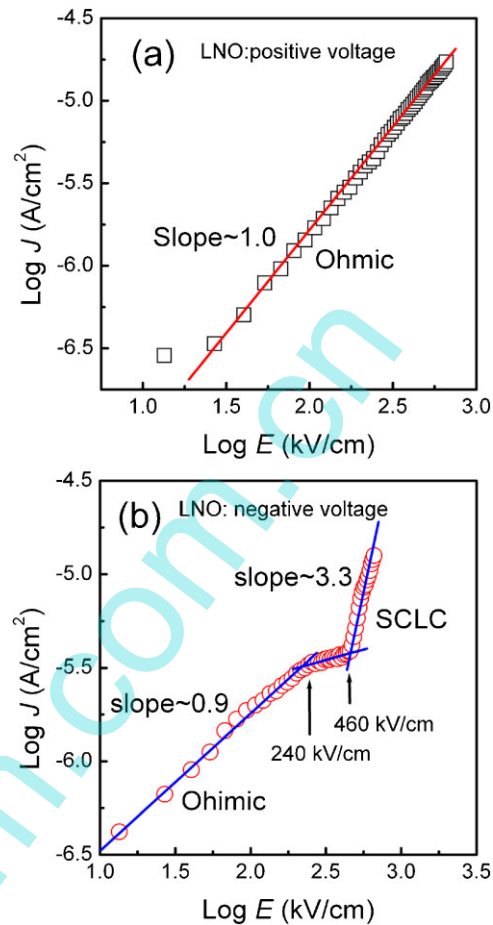
BFMO/STO bilayered thin films. The inset shows the schematic illustration of the thin film capacitor. The polarization hysteresis loop was observed under about  $330 \text{ kV cm}^{-1}$ , giving saturation polarization ( $2P_s$ ), remnant polarization ( $2P_r$ ) and coercive electric field ( $2E_c$ ) values of  $6.2 \mu\text{C cm}^{-2}$ ,  $1.3 \mu\text{C cm}^{-2}$ , and  $80 \text{ kV cm}^{-1}$ , respectively.

Figure 3 shows the leakage current density as a function of applied electric field for BFMO/STO bilayered thin films on a LNO buffered Si(100) substrate at room temperature. The voltage was swept from 0 to 10 V, then from 0 to  $-10 \text{ V}$ . We define the positive bias as positive voltage applied to bottom LNO electrode, while negative bias means positive voltage applying to top Au electrode. The films show leakage current density in the order of  $10^{-5} \text{ A cm}^{-2}$  in the whole electric field region and the lowest leakage current density was about  $7.07 \times 10^{-8} \text{ A cm}^{-2}$ . This low leakage current may be due to two reasons: one reason is the substitution of Mn in Fe site reducing the valence fluctuation between  $\text{Fe}^{3+}$  and  $\text{Fe}^{2+}$ , which can be observed in Mn-doped  $\text{BiFeO}_3$  thin films [21, 22], and the other reason is the existence of STO layer, which is a good insulator. It is obvious that the leakage current density versus applied electric field ( $J$ - $E$ ) curve is asymmetrical in the positive and negative region. One possible reason is the fact that the top (Au) and bottom (LNO) electrodes have different electron affinities and work functions. Another possible reason is the asymmetric internal fields near the film/electrode interfaces formed due to the accumulation of oxygen vacancies or other defects [23], and the third reason could be attributed to the difference in resistivity of BFMO and STO layers.

In order to analyze the leakage conduction behavior of the Au/BFMO/STO/LNO thin-film capacitor, Fig. 4a and b plot the  $\log J$  versus  $\log E$  curves of positive and negative bias applied to LNO electrode, respectively. In Fig. 4a, the plot shows a linear fit in the whole electric field region, where the slope ( $\alpha = \log J / \log E$ ) is calculated to be 1. This indicates a linear Ohmic conduction between Au/BFMO/STO interfaces, which is dominated by thermally stimulated



**Figure 3**  $J$ - $E$  curves of Au/BFMO/STO/LNO thin-film capacitor with positive and negative bias applied to LNO electrode.



**Figure 4** (a) Plot of  $\log J$  versus  $\log E$  for Au/BFMO/STO/LNO thin-film capacitor with positive bias applied to LNO electrode, (b) plot of  $\log J$  versus  $\log E$  for Au/BFMO/STO/LNO thin-film capacitor with negative bias applied to LNO electrode.

free electrons. The leakage current for Ohmic conduction can be expressed by the following equation [24]:

$$J = qN_e\mu E, \quad (1)$$

where  $q$  is the electron charge,  $N_e$  the density of free charge carriers,  $E$  the electric field intensity. While in Fig. 4b, the plot can be fitted well by linear segments with different slopes. At a low electric field region ( $< 230 \text{ kV cm}^{-1}$ ), the slope  $\alpha$  is close to 1 ( $\alpha \sim 0.9$ ), indicating a linear Ohmic conduction between BFMO/STO/LNO interface. At a sufficiently high-applied electric field region ( $> 460 \text{ kV cm}^{-1}$ ), the density of free electrons due to carrier injection becomes greater than the density of thermally stimulated free electrons. Then the current density follows the space-charge-limited conduction (SCLC) mechanism [25]. The current density for SCLC is described by the following equation [26]:

$$J_{\text{SCLC}} = \frac{9\mu\epsilon_0 K v^2}{8d^3}, \quad (2)$$

where  $\mu$  is the carrier mobility and  $d$  the sample thickness. This limitation arises from a current impeding space charge forming as charges and injected into the film from the LNO electrode at a rate faster than that they can travel through the film. The change of the slope from 0.9 to 3.3 indicates a transition of the conduction mechanism from Ohmic to SCLC with increasing electric field strength for LNO/STO interface.

**4 Conclusions** BFMO/STO bilayered thin films have been fabricated on LNO buffered Si(100) substrate by a CSD. The XRD result showed that the film has a hexagonal perovskite structure and the RMS roughness determined by AFM is about 14.5 nm. The room temperature ferroelectricity was observed for the BFMO/STO bilayered thin films. The leakage current behaviors of the Au/BFMO/STO/LNO thin-film capacitor could be considered as follows: Ohmic conduction dominated for Au/BFMO/STO interface when positive bias is applied to the LNO electrode, while the conduction mechanism changes from Ohmic conduction to SCLC for BFMO/STO/LNO interface with increasing negative bias applied to the LNO electrode.

**Acknowledgements** This work was supported by the National Natural Science Foundation of China (Grant Nos. 10774030, 11032010, and 11202054), the Guangdong Provincial Natural Science Foundation of China (Grant Nos. 8151009001000003 and 10151009001000050), and the Guangdong Provincial Educational Commission of China (Grant No. 2012KJCX0044).

## References

- [1] R. Ramesh and N. A. Spaldin, *Nature Mater.* **6**, 21 (2007).
- [2] G. Catalan and J. F. Scott, *Adv. Mater.* **21**, 2463 (2009).
- [3] G. He, Y. Zhang, C. Peng, and X. M. Li, *Appl. Surf. Sci.* **283**, 532 (2013).
- [4] Y. W. Long, T. Kawakami, W. T. Chen, T. Saito, T. Watanuki, Y. Nakakura, Q. Q. Liu, C. Q. Jin, and Y. C. Shimakawa, *Chem. Mater.* **24**, 2235 (2012).
- [5] Y. P. Liu, H. R. Fuh, and Y. K. Wang, *J. Phys. Chem. C* **116**, 18032 (2012).
- [6] C. A. Triana, D. A. Landínez Téllez, J. Arbey Rodríguez, F. Fajardo, and J. Roa-Rojas, *Mater. Lett.* **82**, 116 (2012).
- [7] Y. Du, Z. X. Cheng, S. X. Dou, X. L. Wang, H. Y. Zhao, and H. Kimura, *Appl. Phys. Lett.* **97**, 122502 (2010).
- [8] Y. Du, Z. X. Cheng, H. Y. Zhao, H. Kimura, P. Zhang, Z. P. Guo, and X. L. Wang, *Curr. Appl. Phys.* **11**, s236, (2011).
- [9] H. Y. Zhao, H. Kimura, Z. X. Cheng, X. L. Wang, and T. Nishida, *Appl. Phys. Lett.* **95**, 232904 (2009).
- [10] J. Miao, X. Zhang, Q. Zhan, Y. Jiang, and K.-H. Chew, *Appl. Phys. Lett.* **99**, 062905 (2011).
- [11] P. Liu, Z. X. Cheng, Y. Du, L. Y. Feng, H. Fang, X. L. Wang, and S. X. Dou, *J. Appl. Phys.* **113**, 17D904 (2013).
- [12] J. L. Lai, X. G. Tang, C. B. Ma, R. Li, Q. X. Liu, and Y. P. Jiang, *Integr. Ferroelectr.* **139**, 26 (2012).
- [13] Y. Ye, A. L. Ding, X. G. Tang, and W. G. Luo, *J. Inorg. Mater.* **17**, 125 (2002).
- [14] X. G. Tang, H. L. W. Chan, and A. L. Ding, *Appl. Surf. Sci.* **207**, 63 (2003).
- [15] H. R. Liu and X. Z. Wang, *J. Sol-Gel Sci. Technol.* **47**, 154 (2008).
- [16] L. Bi, A. R. Taussig, H.-S. Kim, L. Wang, G. F. Dionne, D. Bono, K. Persson, G. Ceder, and C. A. Ross, *Phys. Rev. B* **78**, 104106 (2008).
- [17] L. L. Zhu, Y. Chen, K. K. Huang, G. H. Zhang, W. W. Hu, H. M. Yuan, H. B. Chang, and S. H. Feng, *Chem. Res. Chin. Univ.* **26**, 707 (2010).
- [18] K. Uusi-Esko, J. Malm, N. Imamura, H. Yamauchi, and M. Karppinen, *Mater. Chem. Phys.* **112**, 1029 (2008).
- [19] V. G. Prokhorov, G. G. Kaminsky, J. M. Kim, Y. J. Yoo, Y. P. Lee, V. L. Svetchnikov, G. G. Levchenko, Yu. M. Nikolaenko, and V. A. Khokhlov, *Low-Temp. Phys.* **38**, 531 (2012).
- [20] K. Uusi-Esko, J. Malm, and M. Karppinen, *Chem. Mater.* **21**, 5691 (2009).
- [21] T. Kawae, Y. Terauchi, H. Tsuda, M. Kumeda, and A. Morimoto, *Appl. Phys. Lett.* **94**, 112904 (2009).
- [22] J. G. Wu, J. Wang, D. Q. Xiao, and J. G. Zhu, *Appl. Surf. Sci.* **257**, 7226 (2011).
- [23] J. Wei and D. S. Xue, *Appl. Surf. Sci.* **258**, 1373 (2011).
- [24] A. Z. Simões, L. S. Cavalcante, F. Moura, E. Longo, and J. A. Varela, *J. Alloys Compd.* **509**, 5326 (2011).
- [25] X. G. Tang, J. Wang, Y. W. Zhang, and H. L. W. Chan, *J. Appl. Phys.* **94**, 5163 (2003).
- [26] G. W. Pabst, L. W. Martin, Y. H. Chu, and R. Ramesh, *Appl. Phys. Lett.* **90**, 072902 (2007).